JOURNAL OF COMPUTATIONAL PHYSICS 84, 114–133 (1989)

Chebyshev Spectral Collocation Methods for Laminar Flow through a Channel Contraction

ANDREAS KARAGEORGHIS AND TIMOTHY N. PHILLIPS

Department of Mathematics, University College of Wales, Aberystwyth SY23 3BZ, United Kingdom

Received June 3, 1988; revised October 19, 1988

A Chebyshev spectral element method is described for solving the Navier–Stokes equations in a channel contraction. The flow region is divided into two semi-infinite elements. The governing equation for the stream function is solved using a Newton linearization. The semi-infinite elements are treated by means of algebraic-type mappings to transform them onto finite domains. The stream function is represented by a double Chebyshev expansion in each element. The coefficients are determined by collocating the linearized equation at each Newton step and imposing C^3 Continuity conditions across the element interface, in a collocation sense. Efficient direct methods based on capacitance matrix ideas are described which take advantage of the structure of the spectral element matrix. Results are presented for Reynolds numbers in the range [0, 200] which are in good agreement with previously published work but requiring fewer degrees of freedom. Only several steps of the Newton process are required to achieve a converged solution. For $\mathrm{Re} \leqslant 120$ the method converges from a zero initial approximation and thereafter continuation in the Reynolds number is used with increments of 10.

1. INTRODUCTION

In this paper the solution of the Navier–Stokes equations for the steady, 2-dimensional laminar flow of an incompressible fluid through an abruptly contracting channel is obtained with a Chebyshev spectral collocation method. The method used here is an extension of the one developed by Phillips and Karageorghis [24] for Stokes flow.

The distinctive feature of a spectral method is the representation of the solution of a differential equation in terms of a truncated series of smooth, global trial functions. The unknowns to be determined in this method are not the values at selected mesh or nodal points as for the finite difference and finite element methods but the coefficients in the series expansion of the solution. The coefficients are determined using either a Galerkin or a collocation formulation (see Gottlieb and Orszag [6]).

There are three choices for the set of trial functions which are used in practice. First, one can choose the eigenfunctions of the differential operator in the equation to be solved, if these exist and are easily computable. For nonlinear problems this is not a viable choice. The second choice is the set of eigenfunctions of a related but

0021-9991/89 $3.00

simpler differential operator. When these are used exponential convergence of the expansion coefficients is only observed when the problem possesses special properties. Finally one can represent the solution in terms of the eigenfunctions of a singular Sturm–Liouville problem.[1] For linear problems possessing smooth solutions this choice yields expansions which can converge faster than any finite power of N^{-1}, where N is the number of functions in the trial space.

For nonlinear differential equations the coefficients in the truncated series may not converge, as N increases, to the coefficients of the exact series solutions even when the solution is smooth. This is because the coefficients in the truncated expansion are determined by solving a finite system of nonlinear algebraic equations whose solution may deviate from the exact coefficients.

In order to address the question of which is the best set of trial functions for nonlinear problems Davies *et al.* [4] and Karageorghis *et al.* [11] consider a 1-dimensional fifth-order boundary value problem which models viscoelastic flows. They compare the performance of beam functions and Chebyshev polynomials with respect to a parameter which controls the level of nonlinearity of the problem. Their results show that the rapid rate of convergence observed for linear problems is maintained when Chebyshev polynomials are used as trial functions. Furthermore, this choice is not sensitive to the level of nonlinearity and produces accurate results with few degrees of freedom. This is contrary to the experience with beam functions in which convergence slows down considerably for highly nonlinear problems, eventually breaking down completely. An interesting point is that the nonlinear system of equations for the Chebyshev coefficients can be solved without the need for parameter continuation if Newton's method is used. Karageorghis [13] obtains similar results when applying the method to 1-dimensional problems in heat transfer.

For 2-dimensional problems spectral methods are most easily implemented when the domain of interest is either rectangular or circular in which case Chebyshev or Fourier series expansions, respectively, are appropriate. The natural choice of spectral expansion functions for a problem defined in a general irregular region is computationally difficult to determine, unwieldy and inefficient to use, and needs to be computed for each new irregular region. This apparent failure of spectral methods has been overcome by means of domain decomposition techniques in certain situations (Orszag [20], Canuto *et al.* [3]). For many problems in computational fluid dynamics the use of spectral methods in conjunction with domain decomposition techniques appears to be attractive since they combine the flexibility of finite element methods with the superior approximation properties of spectral methods (Patera [21], Morchoisne [18], Karageorghis and Phillips [12]). These techniques are known as spectral element methods. They may be viewed as an extreme case of the p-version of the finite element method where one has a small number of

[1] Chebyshev and Legendre polynomials are examples of such eigenfunctions.

elements and the accuracy of the approximation is improved by increasing the degree of the trial functions.

In this study spectral domain decomposition techniques are used to investigate the laminar flow through an abruptly contracting channel. The spectral element method is quite naturally applied to this problem by dividing the flow region into two semi-infinite domains as shown in Fig. 1. There are two ways in which the semi-infinite elements may be treated: domain truncation or domain mapping. The former technique involves truncating each of the semi-infinite elements at a finite distance from the contraction and has been extensively used in computational fluid dynamics for all types of discretization procedures. The alternative, algebraic-type mappings, is used to transform each of the semi-infinite elements onto finite ones through a transformation of the coordinate in the semi-infinite direction (Grosch and Orszag [7], Boyd [1]). An advantage of mapping techniques is that it is unnecessary to impose boundary conditions at a large but finite distance from the contraction. It is this latter approach which is pursued in the present paper because it circumvents the difficulty of choosing where to truncate the domain.

The spectral element method produces systems of algebraic equations for the expansion coefficients which are block tridiagonal in which the blocks are full. This fact is exploited by Phillips and Karageorghis [24] who use the capacitance matrix method [2] originally devised for finite difference discretizations to invert the spectral element matrix. This method is used here to solve the equations which result from a Newton linearization of the Navier–Stokes equations.

Efficient inversion of the matrices associated with spectral domain decomposition methods have been the subject of other recent papers. Patera [22] presents a direct fast solver for spectral element discretizations of separable elliptic equations on rectangularly decomposable domains. Macaraeg and Streett [16] have adapted an influence matrix technique to spectral patching methods.

The spectral element method described in this paper requires a small number of Newton steps to produce a converged solution. A comparison with the work of Dennis and Smith [5] shows good agreement between the sets of results in terms of stream function contours and behaviour of the salient corner vortex with Reynolds number. For Stokes flow improved solutions around the reentrant corner are obtained using expansions based on the known asymptotic form of the singularity at the corner.

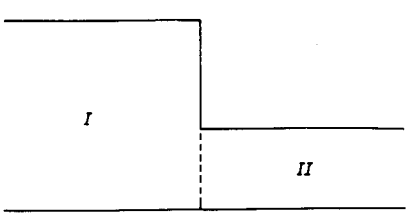

FIG. 1. Geometry of the channel contraction.

2. The Governing Equations

We consider the steady laminar flow of an incompressible fluid through an abruptly contracting channel with walls at $y = \pm 1$ for $x < 0$, $y = \pm\alpha$ for $x > 0$ and $\alpha \leqslant |y| \leqslant 1$ for $x = 0$. The flow is assumed to be symmetric about the centre line $y = 0$ so that only the upper half of the channel need be considered.

In terms of non-dimensional variables the incompressible Navier–Stokes equations are

$$(\mathbf{v} \cdot \nabla)\mathbf{v} = -\nabla p + (\mathrm{Re})^{-1}\nabla^2 \mathbf{v}, \tag{2.1}$$

$$\nabla \cdot \mathbf{v} = 0, \tag{2.2}$$

where $\mathbf{v} = (u, v)$ is the velocity vector, p is the pressure, and Re is the Reynolds number. The introduction of a stream function, $\psi(x, y)$, defined by

$$u = -\frac{\partial \psi}{\partial y}, \qquad v = \frac{\partial \psi}{\partial x}, \tag{2.3}$$

means that the continuity equation (2.2) is automatically satisfied and (2.1) becomes

$$\nabla^4 \psi - \mathrm{Re}\left[\frac{\partial \psi}{\partial y}\frac{\partial}{\partial x}(\nabla^2 \psi) - \frac{\partial \psi}{\partial x}\frac{\partial}{\partial y}(\nabla^2 \psi)\right] = 0. \tag{2.4}$$

On the upper channel wall we have no-slip constraints. The symmetry conditions along the centre of the channel, $y = 0$, are

$$\psi = \frac{\partial^2 \psi}{\partial y^2} = 0. \tag{2.5}$$

We impose Poiseuille flow upstream and downstream of the constriction which means that

$$\psi \to g(y) \qquad \text{as} \quad x \to -\infty, \tag{2.6}$$

$$\psi \to g(y/\alpha) \qquad \text{as} \quad x \to \infty, \tag{2.7}$$

where

$$g(y) = \tfrac{1}{2} y(3 - y^2).$$

The governing equation (2.4) is nonlinear and is solved iteratively using a Newton-type method to linearize it (Phillips [23]). Let us rewrite (2.4) as

$$L(\psi) = 0, \tag{2.8}$$

where L is a nonlinear operator. Suppose that ψ^* is some approximation to the

solution of (2.8). We replace L by its linearization about ψ^* and then solve the linearized problem

$$L'(\psi^*)\cdot\phi = -L(\psi^*), \tag{2.9}$$

where $L'(\psi^*)$ is the Frechet derivative of L at ψ^* defined by

$$L'(\psi)\cdot\phi = \nabla^4\phi - \mathrm{Re}\left[\frac{\partial\psi}{\partial y}\frac{\partial}{\partial x}(\nabla^2\phi) - \frac{\partial\psi}{\partial x}\frac{\partial}{\partial y}(\nabla^2\phi) + \frac{\partial}{\partial x}(\nabla^2\psi)\frac{\partial\phi}{\partial y} - \frac{\partial}{\partial y}(\nabla^2\psi)\frac{\partial\phi}{\partial x}\right]. \tag{2.10}$$

The new approximation to the solution is thus $\psi^* + \phi$. This completes a single Newton step and is repeated until convergence is reached.

3. Spectral Collocation Method

The spectral element method can be naturally applied to the problem considered here by dividing the flow region into two semi-infinite regions as shown in Fig. 1. There are essentially three ways of treating the semi-infinite domains and choosing appropriate trial functions:

(a) using a Chebyshev–Laguerre representation in the original semi-infinite domain;

(b) truncating the domain and using a Chebyshev–Chebyshev representation;

(c) mapping the domain onto a finite one and using a Chebyshev–Chebyshev representation.

A comparison of these choices for Stokes problems is made in Karageorghis and Phillips [12]. Their study concluded that the choice (c) gave the most promising results. Therefore in this paper we restrict our attention to the domain mapping techniques which were first used within a spectral context by Grosch and Orszag [7] for 1-dimensional problems.

The subregions I and II (see Fig. 1) are each mapped onto a finite rectangle by means of an algebraic-type mapping. If we define subregion I by the set of points

$$R_{\mathrm{I}} = \{(x, y): -\infty < x \leqslant 0, 0 \leqslant y \leqslant 1\},$$

then under the algebraic mapping

$$z = \frac{-x}{(x + L_{\mathrm{I}})}, \qquad L_{\mathrm{I}} < 0, \tag{3.1}$$

R_I is mapped onto V_I where

$$V_I = \{(z, y): -1 \leqslant z \leqslant 0, 0 \leqslant y \leqslant 1\}.$$

Similarly, subregion II is mapped onto V_{II} where

$$V_{II} = \{(z, y): 0 \leqslant z \leqslant 1, 0 \leqslant y \leqslant \alpha\}$$

under the algebraic mapping

$$z = \frac{x}{(x + L_{II})}, \qquad L_{II} > 0. \tag{3.2}$$

The mapped regions are shown in Fig. 2. The parameters L_I and L_{II} appearing in Eqs. (3.1) and (3.2) are known as mapping parameters.

In each of the regions V_I and V_{II} the stream function $\psi(z, y)$ is approximated by $\psi^I(z, y)$ and $\psi^{II}(z, y)$, respectively, where

$$\psi^I(z, y) = g(y) + \sum_{m=0}^{M} \sum_{n=4}^{N} a_{mn} T_m^+(z) P_n(y), \tag{3.3}$$

$$\psi^{II}(z, y) = g(y/\alpha) + \sum_{m=0}^{K} \sum_{n=4}^{N} b_{mn} T_m^*(z) P_n(y/\alpha), \tag{3.4}$$

where

$$T_m^+(z) = T_m(2z + 1), \; T_m^*(z) = T_m(2z - 1) \tag{3.5}$$

and $T_m(y)$ are the classical Chebyshev polynomials defined on $[-1, 1]$. The trial functions in the y-direction are modified Chebyshev polynomials defined so that $\psi^I(z, y)$ and $\psi^{II}(z, y)$ automatically satisfy the boundary conditions along the top of the channel and the axis of symmetry. According to this specification we take

$$P_n(y) = T_n^*(y) + \alpha_n T_3^*(y) + \beta_n T_2^*(y) + \gamma_n T_1^*(y) + \delta_n T_0^*(y) \tag{3.6}$$

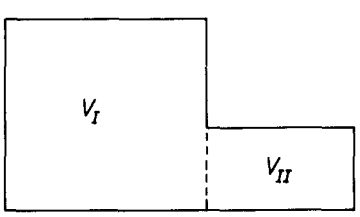

FIG. 2. Mapping of semi-infinite elements onto finite ones.

where

$$\alpha_n = \{-n^2 - \tfrac{1}{2}(-1+(-1)^n) + (-1)^n n^2(n^2-1)/3\}/32,$$
$$\beta_n = 6\alpha_n - (-1)^n n^2(n^2-1)/12,$$
$$\gamma_n = -\alpha_n + \tfrac{1}{2}(-1+(-1)^n),$$
$$\delta_n = -1 - \alpha_n - \beta_n - \gamma_n.$$

At each stage of the Newton process, the linearized equation (2.9) is solved using the spectral collocation method in the mapped domain. Note that derivatives of the stream function with respect to x are transformed into derivatives with respect to z in region V_{I} as

$$\frac{\partial^q \psi^{\mathrm{I}}}{\partial x^q} = (-L_{\mathrm{I}})^{-q} \sum_{j=1}^{q} c_j^{(q)} (1+z)^{q+j} \frac{\partial^j \psi^{\mathrm{I}}}{\partial z^j}, \qquad q = 1, 2, 3, 4, \tag{3.7}$$

where the coefficients $c_j^{(q)}$ can be evaluated from the recurrence relation

$$(q+j)\, c_j^{(q)} + c_{j-1}^{(q)} = c_j^{(q+1)},$$
$$c_1^{(q)} = q!$$

A similar process is performed in region V_{II} for the x-derivatives of ψ^{II}. The transformed equation is collocated at certain points in the mapped regions related to the extrema of the Chebyshev polynomial of highest degree used in the representations (3.3) and (3.4).

Suppose that at the beginning of a Newton step we have approximations a_{mn}^* and b_{mn}^* to coefficients of ψ^{I} and ψ^{II}, respectively, then the collocation method applied to the transformed version of (2.9) results in a linear system of algebraic equations for $(\delta a)_{mn}$ and $(\delta b)_{mn}$, the coefficients of ϕ in V_{I} and V_{II}, respectively. Thus, for example, in region V_{I} an equation of the form

$$\sum_{m=0}^{M} \sum_{n=4}^{N} (\delta a)_{mn} [A_{mn}(z, y) - \mathrm{Re}\, B_{mn}(z, y, \mathbf{a}^*)] = \mathrm{Re}\, C(z, y, \mathbf{a}^*), \tag{3.8}$$

is collocated at certain points. Here A_{mm}, B_{mn}, and C are known functions of their arguments and $\mathbf{a}^*$ is the vector whose components are a_{mn}^*. A corresponding equation is valid in V_{II}.

The solutions in the two regions are patched by imposing C^3 continuity conditions in a collocation sense across the interface. These are the natural boundary conditions for the associated variational principle. Thus, with respect to the original domain we require

$$\psi^{\mathrm{I}}(0, y) = \begin{cases} \psi^{\mathrm{II}}(0, y), & 0 \leqslant y \leqslant \alpha, \\ 1, & \alpha \leqslant y \leqslant 1, \end{cases} \tag{3.9}$$

$$\frac{\partial \psi^{\mathrm{I}}}{\partial x}(0, y)=\begin{cases}\dfrac{\partial \psi^{\mathrm{II}}}{\partial x}(0, y) & 0 \leqslant y \leqslant \alpha, \\ 0, & \alpha \leqslant y \leqslant 1,\end{cases} \tag{3.10}$$

$$\frac{\partial^2 \psi^{\mathrm{I}}}{\partial x^2}(0, y)=\frac{\partial^2 \psi^{\mathrm{II}}}{\partial x^2}(0, y), \qquad 0 \leqslant y \leqslant \alpha, \tag{3.11}$$

$$\frac{\partial^3 \psi^{\mathrm{I}}}{\partial x^3}(0, y)=\frac{\partial^3 \psi^{\mathrm{II}}}{\partial x^3}(0, y), \qquad 0 \leqslant y \leqslant \alpha, \tag{3.12}$$

at certain points across the interface. The derivatives with respect to x are transformed into derivatives with respect to z to obtain the associated interface conditions in the mapped domain. Therefore at each Newton step we insist that $\psi^* + \phi$ satisfies these conditions at the element interface.

At each stage of the iterative process there are a total of $(M+K+2)(N-3)$ coefficients to be determined. This is verified by inspection of (3.3) and (3.4). An equal number of equations needs to be generated. Consider the following sets of collocation points

$$T_1 = \{(x_i^{\mathrm{I}}, y_j^{\mathrm{I}}): 3 \leqslant i \leqslant M, 2 \leqslant j \leqslant N-2\},$$
$$T_2 = \{(x_i^{\mathrm{II}}, y_j^{\mathrm{II}}): 3 \leqslant i \leqslant M, 2 \leqslant j \leqslant N-2\},$$
$$T_3 = \{(0, y_j^{\mathrm{I}}): 2 \leqslant j \leqslant N-2\},$$
$$T_4 = \{(0, y_j^{\mathrm{II}}): 2 \leqslant j \leqslant N-2\},$$

where we define

$$x_i^{\mathrm{I}} = -\frac{1}{2}\left\{1+\cos \pi\left(1-\frac{i}{N}\right)\right\}, \qquad x_i^{\mathrm{II}} = -x_i^{\mathrm{I}},$$

$$y_j^{\mathrm{I}} = \frac{1}{2}\left\{1+\cos \pi\left(1-\frac{j}{N}\right)\right\}, \qquad y_j^{\mathrm{II}} = \alpha y_j^{\mathrm{I}}.$$

We collocate (3.8) at points in T_1 and the corresponding equation in V_{II} at points in T_2. The interface conditions (3.9) and (3.10) are collocated at points in T_3 and (3.11) and (3.12) at points in T_4. This choice yields the correct number of equations to determine the coefficients of ϕ. The coefficients of the updated representations are therefore $a_{mn}^* + (\delta a)_{mn}$ and $b_{mn}^* + (\delta b)_{mn}$. The Newton process is then repeated until convergence is reached.

The omission of the extreme Chebyshev collocation points in choosing T_1, T_2, T_3, and T_4 means that near the boundaries and element interface the approximations ψ^{I} and ψ^{II} are influenced more by the boundary conditions and interface continuity conditions than by the differential equation. In the next section we describe an efficient method for solving the linear system of equations obtained at each Newton step.

4. A Capacitance Matrix Method for Solving the Spectral Collocation Equations

At each Newton step there results a system of linear equations for the corrections to the expansion coefficients of the form

$$\left[\begin{array}{c|c} A & 0 \\ \hline C & \\ \hline D & \\ \hline 0 & B \end{array}\right] \left[\begin{array}{c} \delta\mathbf{a} \\ \hline \\ \hline \\ \delta\mathbf{b} \end{array}\right] = \left[\begin{array}{c} \mathbf{r} \\ \hline \mathbf{s} \\ \hline \mathbf{t} \end{array}\right]. \tag{4.1}$$

The dimension of the system in (4.1) is $n_1 + 2n_2 + n_3$, where

$$n_1 = (M-1)(N-3),$$
$$n_2 = 2(N-3),$$
$$n_3 = (K-1)(N-3).$$

The first n_1 rows of (4.1) correspond to the collocation of (3.8) at points in T_1 while the last n_3 rows correspond to collocation of the analogous equation in V_{II} at points in T_2. The rows corresponding to C represent collocation of the interface conditions (3.9) and (3.10) in T_3 while those corresponding to D represent collocation of (3.11) and (3.12) in T_4.

For the Stokes problem Karageorghis and Phillips [12] solve the system (4.1) using a Crout factorization technique from the NAG Library [19]. Thus $k(n_1 + 2n_2 + n_3)^3$ operations are needed to obtain the solution where k is some constant. However, in this approach no advantage is taken of the two blocks of zeros in the coefficient matrix of (4.1). The capacitance matrix method was originally developed by Buzbee *et al.* [2] for the finite difference method in order to take account of the structure of the coefficient matrix in constructing solution techniques for problems in rectangularly decomposable domains. Phillips and Karageorghis [24] extended the idea to spectral discretizations of the Stokes problem and here we develop the technique for the Navier–Stokes equations. An advantage of using such a technique is that we are not so restricted in the size of problem that we can solve. Furthermore, capacitance matrix methods are efficient in terms of storage locations and computational time.

To demonstrate this method we rewrite (4.1) in the partitioned form:

$$\left[\begin{array}{c|c|c} E & F & 0 \\ \hline G & H & R \\ \hline 0 & P & Q \end{array}\right] \left[\begin{array}{c} \mathbf{x} \\ \hline \mathbf{y} \\ \hline \mathbf{z} \end{array}\right] = \left[\begin{array}{c} \mathbf{r} \\ \hline \mathbf{s} \\ \hline \mathbf{t} \end{array}\right]. \tag{4.2}$$

The square matrices E, H, and Q are of order n_1, $2n_2$, and n_3, respectively. To apply the capacitance matrix method (4.2) is written in the component form suggested by the partitioning, i.e.,

$$E\mathbf{x} + F\mathbf{y} \qquad = \mathbf{r}, \tag{4.3}$$

$$G\mathbf{x} + H\mathbf{y} + R\mathbf{z} = \mathbf{s}, \tag{4.4}$$

$$P\mathbf{y} + Q\mathbf{z} = \mathbf{t}. \tag{4.5}$$

We write $\mathbf{x}$ and $\mathbf{z}$ in terms of $\mathbf{y}$ by premultiplying (4.3) and (4.5) by the inverses of E and Q, respectively, i.e.,

$$\mathbf{x} = E^{-1}\mathbf{r} - E^{-1}F\mathbf{y}, \qquad \mathbf{z} = Q^{-1}\mathbf{t} - Q^{-1}P\mathbf{y}.$$

Eliminating $\mathbf{x}$ and $\mathbf{z}$ from (4.4) we obtain the following system for $\mathbf{y}$:

$$(H - GE^{-1}F - RQ^{-1}P)\mathbf{y} = \mathbf{s} - GE^{-1}\mathbf{r} - RQ^{-1}\mathbf{t}, \tag{4.6}$$

where the coefficient matrix on the left-hand side of (4.6) is known as the capacitance matrix. The order of this system is $2n_2$ which is much smaller than that of the original system (4.1) and can be efficiently solved using the Crout factorization technique.

Most of the work in this technique is associated with the inversion of the matrices E and Q together with the capacitance matrix. The determination of $E^{-1}\mathbf{r}$ and $E^{-1}F$ requires the solution of (n_2+1) systems of order n_1 with coefficient matrix E. This requires $k(n_1)^3 + (n_2+1)(n_1)^2$ operations. Similarly $Q^{-1}\mathbf{t}$ and $Q^{-1}P$ are calculated by solving (n_2+1) systems of order n_3 at a cost of $k(n_3)^3 + (n_2+1)(n_3)^2$ operations. The solution of the capacitance system (4.6) requires $8k(n_2)^3 + (n_2)^2$ operations. Thus the capacitance matrix method requires $O(n_1 n_3(n_1+n_3))$ fewer operations to solve (4.2) than the number needed to invert the original system. The method also produces a saving of $O(n_1 n_3)$ storage locations.

5. Treatment of the Stokesian Reentrant Corner Singularity

The problem being considered possesses a singularity at the reentrant corner $(0, \alpha)$. This has been the subject of several studies for both the Stokes [9, 14, 17, 25] and Navier–Stokes [8, 15] problems. In a vicinity of the reentrant corner we may require hundreds of terms in the expansions (3.3) and (3.4) to obtain accurate solutions there due to the presence of the singularity. For the Stokes problem the asymptotic behaviour of the solution at and near a reentrant corner is known [17]. Holstein and Paddon [9, 10] incorporate this known asymptotic form of the singularity into a finite difference method of solution. Phillips [25] uses the spectral element method with expansions in Papkovich–Fadle eigenfunctions to solve the Stokes problem. The solution is then post-processed to determine the coefficients in the asymptotic expansion near the corner. The method is successful because at a sufficient distance from the corner the spectral representations converge rapidly since the effect of the singularity does not penetrate far into the interior of the region. These ideas are used to post-process the double Chebyshev solutions obtained for the Stokes problem in this paper.

In the rest of this section we describe briefly the post-processing technique. Define a neighborhood, S, of the reentrant corner by

$$S = \{(r, \theta): 0 \leqslant r \leqslant R,\ -3\pi/4 \leqslant \theta \leqslant 3\pi/4\},$$

where $r^2 = x^2 + (y-\alpha)^2$ and θ is the polar angle (see Fig. 3). The biharmonic equation may be written as a second-order system in polar coordinates [26],

$$\left(r\frac{\partial}{\partial r}\right)^2 \mathbf{\Psi} - A\mathbf{\Psi} = \mathbf{0}, \tag{5.1}$$

where

$$A = \begin{bmatrix} 0 & 1 \\ -(\partial^2/\partial\theta^2 + 1)^2 & -2(\partial^2/\partial\theta^2 - 1) \end{bmatrix}, \tag{5.2}$$

and

$$\mathbf{\Psi}^{\mathrm{T}} = (\psi_1, \psi_2) = \left(\frac{\psi - 1}{r}, \left(r\frac{\partial}{\partial r}\right)^2\left(\frac{\psi - 1}{r}\right)\right). \tag{5.3}$$

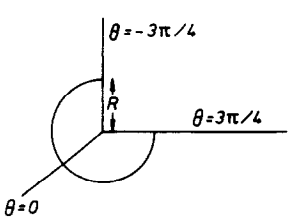

FIG. 3. Reentrant corner sector.

Since the solution of the biharmonic equation in a sector admits a separation of variables solution [17] we write Ψ in the form

$$\Psi(r, \theta) = \sum_{k=1}^{\infty} d_k r^{\sqrt{\lambda_k}} \mathbf{u}_k(\theta). \tag{5.4}$$

Substitution of (5.4) into (5.1) yields

$$A\mathbf{u}_k = \lambda_k \mathbf{u}_k, \tag{5.5}$$

where $\mathbf{u}_k = (u_k, \lambda_k u_k)^T$. The no-slip boundary conditions on the arms $\theta = \pm 3\pi/4$ of the sector mean that u_k and λ_k are given by

$$u_k(\theta) = \begin{cases} \cos\frac{3\pi}{4}(\sqrt{\lambda_k}-1)\cos(\sqrt{\lambda_k}+1)\theta - \cos\frac{3\pi}{4}(\sqrt{\lambda_k}+1)\cos(\sqrt{\lambda_k}-1)\theta, & k \text{ odd}, \\ \sin\frac{3\pi}{4}(\sqrt{\lambda_k}-1)\sin(\sqrt{\lambda_k}+1)\theta - \sin\frac{3\pi}{4}(\sqrt{\lambda_k}+1)\sin(\sqrt{\lambda_k}-1)\theta, & k \text{ even}, \end{cases}$$

$$\sin\frac{3\pi}{2}\sqrt{\lambda_k} = (-1)^{k+1}\sqrt{\lambda_k}. \tag{5.7}$$

The first two roots of this transcendental equation are real and the rest occur in conjugate pairs.

The adjoint eigenfunctions, $\mathbf{v}_k$, are given by $\mathbf{v}_k = (v_k, u_k)^T$ with

$$v_k(\theta) = 2u_k''(\theta) + (\lambda_k - 2)\, u_k(\theta),$$

and are biorthogonal to the $\mathbf{u}_k(\theta)$ in the sense that

$$\int_{-3\pi/4}^{3\pi/4} \mathbf{v}_m^T(\theta)\, A\mathbf{u}_k(\theta)\, d\theta = 0, \qquad \text{for} \quad m \neq k. \tag{5.8}$$

Using (5.5) one can show that

$$\int_{-3\pi/4}^{3\pi/4} \mathbf{v}_m^T(\theta)\, \mathbf{u}_k(\theta)\, d\theta = c_k\, \delta_{k,m}, \tag{5.9}$$

where

$$c_k = \begin{cases} 3(\lambda_k - 1)\pi + 2\cos\left(\frac{3\pi}{2}\sqrt{\lambda_k}\right), & k \text{ odd}, \\ 3(\lambda_k + 1)\pi - 2\cos\left(\frac{3\pi}{2}\sqrt{\lambda_k}\right), & k \text{ even}. \end{cases}$$

In the post-processing technique (5.4) is assumed to be valid in S with the infinite sum replaced by a finite one of L terms, say. The unknown coefficients, d_k, in this

expansion are determined by matching this expansion with the double Chebyshev representation along the circumference of S. The coefficients are given by

$$d_k = \frac{1}{c_k R^{1+\sqrt{\lambda_k}}} \int_{-3\pi/4}^{3\pi/4} \{ p(R, \theta)\, v_k(\theta) + q(R, \theta)\, u_k(\theta) \}\, d\theta, \tag{5.10}$$

for $k = 1, 2, ..., L$, where

$$p(r, \theta) = \psi^R - 1, \qquad q(r, \theta) = r^2 \frac{\partial^2 \psi^R}{\partial r^2} - r \frac{\partial \psi^R}{\partial r} + \psi^R - 1,$$

and

$$\psi^R(x, y) = \begin{cases} \psi^{\mathrm{I}}(x, y), & \text{if } x \leqslant 0, \\ \psi^{\mathrm{II}}(x, y), & \text{if } x > 0. \end{cases}$$

All the functions on the right-hand side of (5.10) are known. However, the integral cannot be evaluated analytically because of the complicated form of the integrand and so the trapezoidal rule is used. Once the coefficients d_k, $k = 1, 2, ..., L$ have been determined the solution within S is then given by

$$\psi^s(r, \theta) = 1 + \sum_{k=1}^{L} d_k r^{1+\sqrt{\lambda_k}} u_k(\theta). \tag{5.11}$$

Outside S the solution is given by ψ^R.

6. Numerical Results

Navier–Stokes Equations

Results are presented for laminar flow ($0 \leqslant \mathrm{Re} \leqslant 200$) through a 2 : 1 channel contraction. A comparison is made with the work of Dennis and Smith [5] who use a finite difference method with an extremely fine mesh. The performance of the spectral algorithm with respect to the degree of the Chebyshev representation, the mapping parameters, and the Reynolds number is examined.

The Newton process is terminated when the maximum difference between consecutive values of the expansion coefficients is less than 10^{-6}. For relatively few degrees of freedom and with a zero initial guess for the coefficients convergence is only achieved for low values of the Reynolds number. In Figs. 4a–d we present contour plots of the stream function for $\mathrm{Re} = 0$, 10, 25, and 50, respectively. Further, even with continuation in Re convergence is not obtained for much higher values of Re before the interelement continuity suffers considerably (see Fig. 4). Efforts to concentrate more collocation points near the element interface by reducing the mapping parameters L_{I} and L_{II} proved only partially successful.

As the number of degrees of freedom is increased convergence and satisfactory

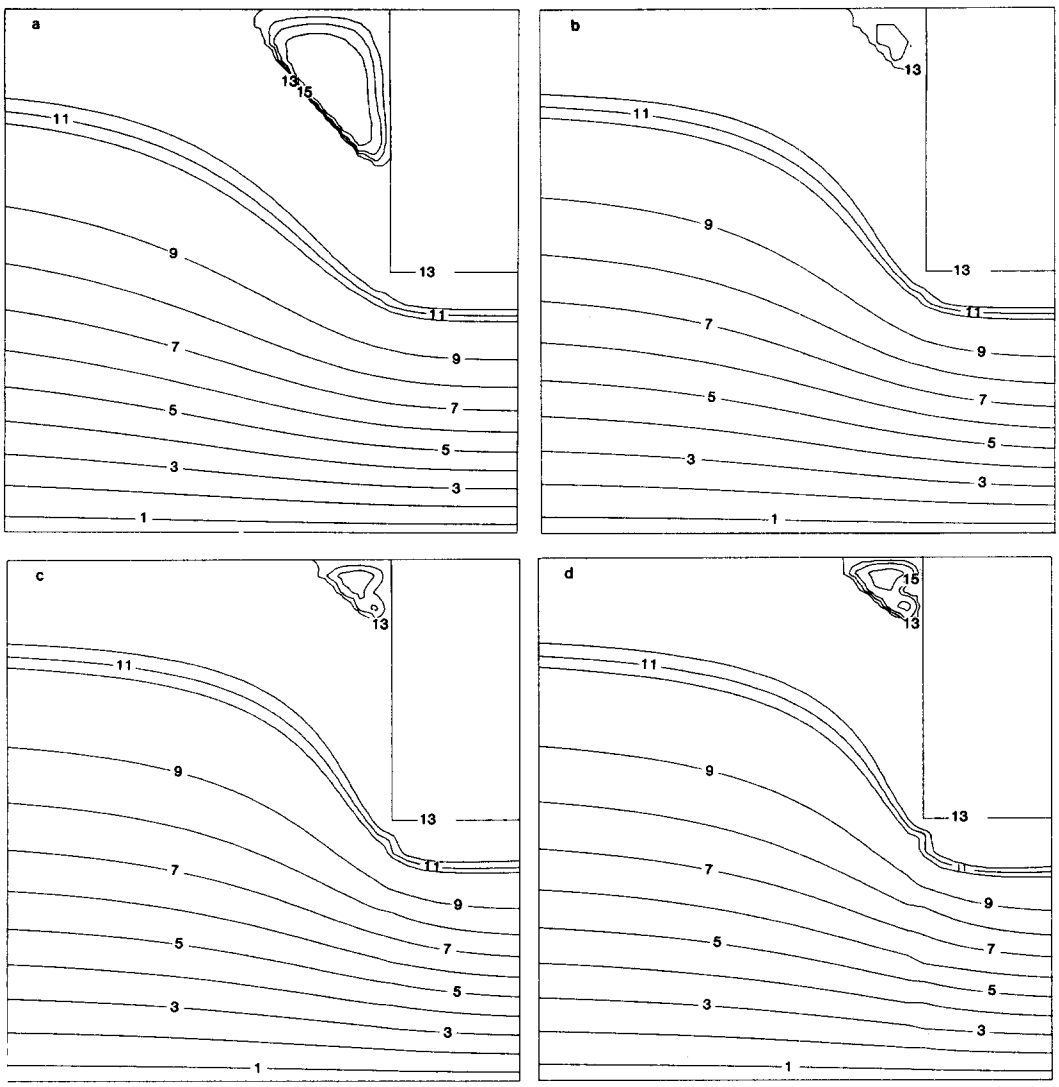

FIG. 4. Contour plots of the stream function obtained with $N = 17$, $M = 16$, $K = 10$ for (a) $\mathrm{Re} = 0$, (b) $\mathrm{Re} = 10$, (c) $\mathrm{Re} = 25$, (d) $\mathrm{Re} = 50$.

interelement continuity is obtained for progressively higher values of the Reynolds number when starting from a zero initial guess for the stream function. For $N = M = K = 25$ no continuation is required for $\mathrm{Re} \leqslant 120$. Only six steps of the Newton process are required to reach convergence. The Jacobian is updated after every step since only a small number of iterations are needed. If a greater number of steps were needed to converge we would update the Jacobian after each of the first few iterations until the solution settled down and subsequently after every two

TABLE I

CPU Times and Storage on an Amdahl 5890-300 Computer Required for Six Newton Iterations for Re = 50

$N = M = K$	Number of degrees of freedom	CPU times (seconds)	Storage (kbytes)
7	64	1.4	129
13	280	15.8	637
19	640	106.5	2456
25	1144	442.3	6976

or three iterations. In Figs. 5a–h we present contour plots of the stream function for Re = 0, 1, 10, 25, 50, 100, and 200, respectively. For $\mathrm{Re} \leqslant 100$ the method is insensitive to the values of the mapping parameters in the proximity of the chosen ones of $L_{\mathrm{I}} = -1.5$ and $L_{\mathrm{II}} = 1.5$. For $\mathrm{Re} > 100$ we found that the interelement continuity depended on the values of the mapping parameters. To obtain a more accurate solution of the problem at the interface more collocation points in the x-direction are concentrated there by simply reducing the values of the mapping parameters. The results of Fig. 5(g) for Re = 150 are with $L_{\mathrm{I}} = L_{\mathrm{II}} = 0.8$ and of Fig. 5(h) for Re = 200 with $L_{\mathrm{I}} = L_{\mathrm{II}} = 0.6$.

The growth of the salient vortex is also investigated. The distance, L_v, between the point where the separation line meets the top of the channel and the salient corner is recorded for different values of Re. A comparison of this length with that obtained by Dennis and Smith [5] is shown in the graph of Fig. 6 for Reynolds numbers in the range $0 \leqslant \mathrm{Re} \leqslant 200$. There is good agreement between the two sets of results. The length L_v decreases gradually from Re = 0 until around Re = 45 and then increases monotonically. Similar observations were made regarding the strength of the salient corner vortex.

TABLE II

Dependence of Coefficients in Asymptotic Expansion on R

R	a_1	a_2	$\mathrm{Re}(a_3)$	$\mathrm{Im}(a_3)$	$\mathrm{Re}(a_4)$	$\mathrm{Im}(a_4)$
0.125	−2.0667	5.9369	0.0514	0.3997	0.2822	0.3522
0.250	−1.9786	6.2491	−0.3178	0.5685	−0.2051	0.2351
0.375	−1.9663	6.3795	−0.3930	0.6014	−0.2759	0.2005
0.500	−1.9814	6.5126	−0.4393	0.6240	−0.3110	0.1844
Kelmanson [14] (320 nodes)	−1.9862	6.5599	−0.4536	0.6292	−0.3114	0.1754

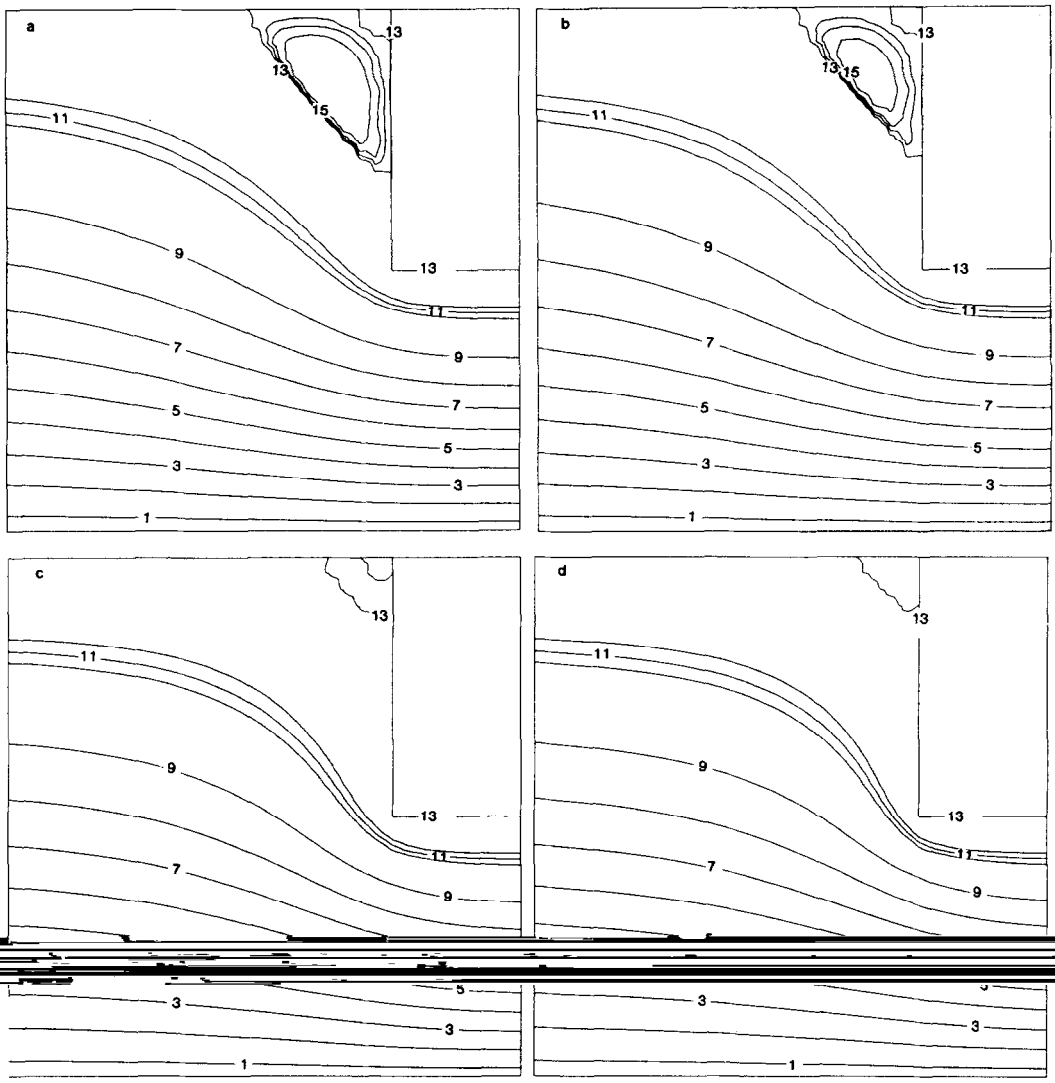

FIG. 5. Contour plots of the stream function obtained with $N = M = K = 25$ for (a) Re = 0, (b) Re = 1, (c) Re = 10, (d) Re = 25, (e) Re = 50, (f) Re = 100, (g) Re = 150, (h) Re = 200.

Finally, we consider the computational requirements of the Chebyshev spectral collocation method. In Table I we show how the CPU time, in seconds, and storage, in kilobytes, varies with the number of degrees of freedom in the case when Re = 50. Unlike finite difference or finite element discretizations the storage requirements increase dramatically with the size of the problem. This is due to the non-sparse structure of the spectral element matrix. At least three times fewer

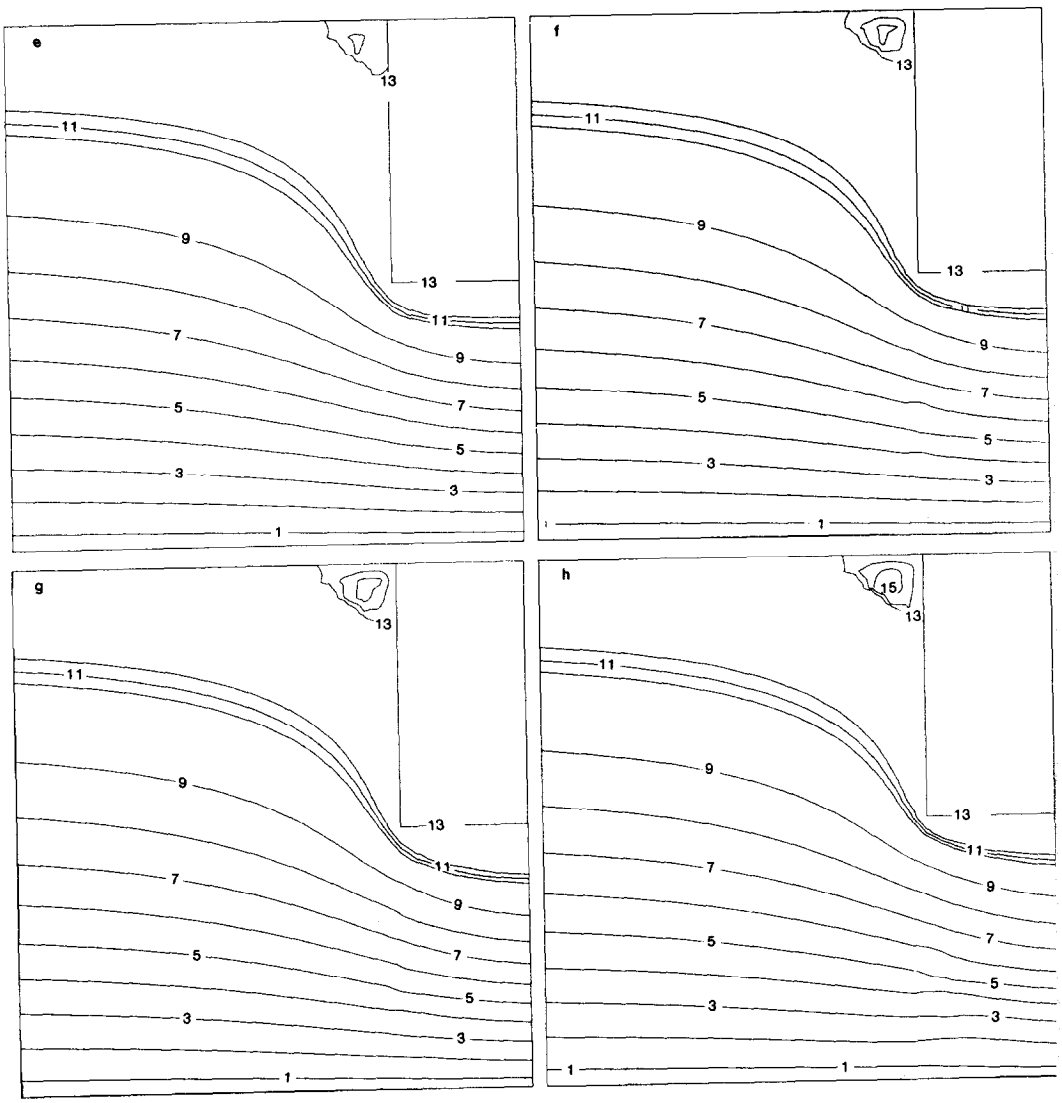

FIG. 5—*Continued*

degrees of freedom are used in this method than the method of Dennis and Smith [5] to obtain comparable results.

All computations were performed on an Amdahl 5890-300 computer located at the University of Manchester Regional Computing Centre.

Stokes Singularity

Here we present results of the post-processing of the Stokes solution obtained with $N = M = 16$, $K = 8$. With this number of degrees of freedom the degradation in

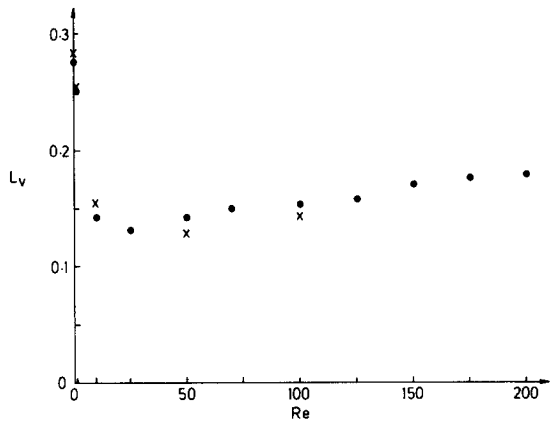

FIG. 6. The dependence of L_v on Reynolds number. Our results (●) are in good agreement with previous calculations [5] (×).

the smoothness of the solution is observed around the reentrant corner due to the presence of a singularity there. The post-processing technique was applied with both six and ten terms in the singular expansions and for different values of the sector radius R. The use of six terms is sufficient to produce smooth contours in the neighbourhood of the singularity. The stream lines before and after post-processing are shown in Figs. 7(a) and (b), respectively. A close-up of the solution around the reentrant corner before and after the post-processing is given in Figs. 7(c) and (d), respectively.

The values of the coefficients in the asymptotic expansion in the region around the singularity are recorded for different values of R and tabluated in Table II. The coefficients are compared with those of Kelmanson [14] who uses a boundary integral formulation which incorporates the correct singular behaviour in the neighbourhood of the singularity. The two sets of coefficients are in good agreement.

7. CONCLUSIONS

The steady laminar flow of an incompressible fluid through a channel contraction is examined. The stream function formulation of the governing Navier–Stokes equations is linearized using Newton's method and solved numerically using a Chebyshev spectral collocation method. The semi-infinite elements are treated using an algebraic-type transformation to map them onto finite rectangles.

The spectral element collocation method for the linearized Navier–Stokes equations results in a system of linear equations with a block tridiagonal structure at each Newton step. Each of these non-zero blocks is a full matrix. The structure of the spectral elements matrix is exploited using a capacitance matrix method. This,

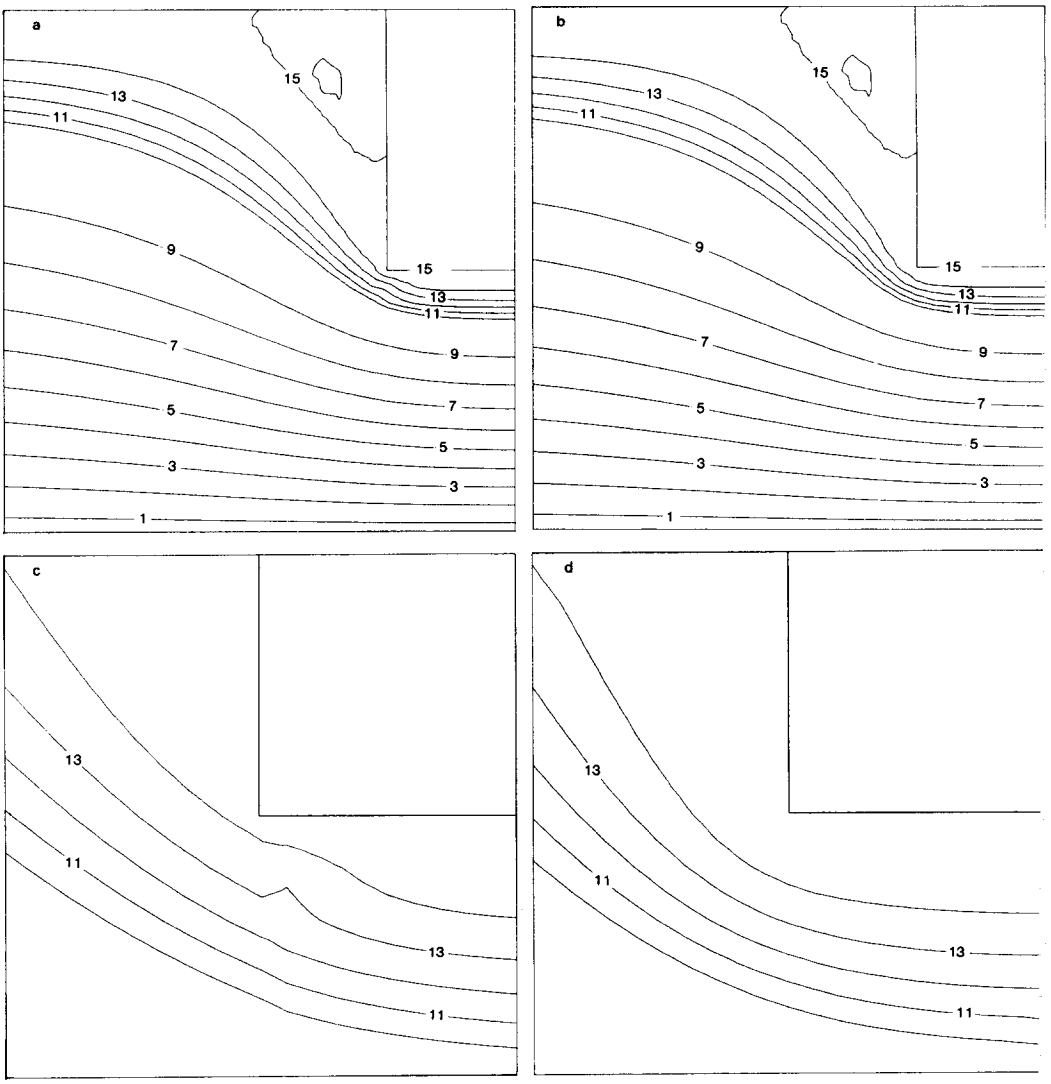

FIG. 7. Contours of the stream function for the Stokes problem (a) before and (b) after post-processing. A magnification of the situation is shown (c) before and (d) after post-processing.

of course, is much more efficient than solving the full system directly without taking into account the inherent matrix structure. The capacitance matrix method also enables us to solve larger systems than is possible with the original method and, as a result, more accurate solutions are obtained. Only a small number of steps in the Newton process is required to reach a converged solution. The results agree qualitatively and quantitatively with previously published work.

For Stokes flow the reentrant corner singularity is treated using a post-processing

technique which incorporates the analytical solution of the problem in a neighbourhood of the corner. This technique improves the quality of the solution around the reentrant corner. The extension of this idea to flows with non-zero Reynolds numbers is presently under investigation.

In this paper we have restricted ourselves to the numerical spectral simulation of laminar flows. The possible extension of the method described in this paper to the non-laminar regime would inevitably require more spatial resolution. This means that efficient iterative methods as opposed to the direct methods considered here would need to be devised to solve the spectral collocation equations in this case.

ACKNOWLEDGMENTS

The authors are grateful to the UK Science and Engineering Research Council for financial support which enabled this work to be performed.

REFERENCES

1. J. P. BOYD, *J. Comput. Phys.* **45**, 43 (1982).
2. B. L. BUZBEE, F. W. DORR, J. A. GEORGE, AND G. H. GOLUB, *SIAM J. Numer. Anal.* **8**, 722 (1971).
3. C. CANUTO, M. Y. HUSSAINI, A. QUARTERONI, AND T. A. ZANG, *Spectral Methods in Fluid Dynamics* (Springer-Verlag, Berlin, 1988).
4. A. R. DAVIES, A. KARAGEORGHIS, AND T. N. PHILLIPS, *Int. J. Num. Methods Eng.* **26**, 647 (1988).
5. S. C. R. DENNIS AND F. T. SMITH, *Proc. Roy. Soc. London A* **372**, 393 (1980).
6. D. GOTTLIEB AND S. A. ORSZAG, *Numerical Analysis of Spectral Methods: Theory and Applications* (SIAM, Philadelphia, 1977).
7. C. E. GROSCH AND S. A. ORSZAG, *J. Comput. Phys.* **25**, 273 (1977).
8. M. M. GUPTA, R. P. MANOHAR, AND B. NOBLE, *Comput. Fluids* **9**, 379 (1981).
9. H. HOLSTEIN AND D. J. PADDON, *J. Non-Newtonian Fluid Mech.* **8**, 81 (1981).
10. H. HOLSTEIN AND D. J. PADDON, in *Numerical Methods for Fluid Dynamics*, edited by K. W. Morton and M. J. Baines (Academic Press, London, 1982).
11. A. KARAGEORGHIS, T. N. PHILLIPS, AND A. R. DAVIES, *Int. J. Num. Methods Eng.* **26**, 805 (1988).
12. A. KARAGEORGHIS AND T. N. PHILLIPS, *J. Comput. Phys.* **80**, 314 (1989).
13. A. KARAGEORGHIS, *Comput. Methods Appl. Mech. Eng.* **70**, 103 (1988).
14. M. A. KELMANSON, *Comput. Fluids* **11**, 307 (1988).
15. H. J. LUGT AND E. W. SCHWIDERSKI, *Proc. Roy. Soc. London A* **285**, 382 (1964).
16. M. MACARAEG AND C. L. STREETT, *Appl. Numer. Math.* **2**, 95 (1986).
17. H. K. MOFFATT, *J. Fluid Mech.* **18**, 1 (1964).
18. Y. MORCHOISNE, in *Spectral Methods for Partial Differential Equations*, edited by R. G. Voigt, D. Gottlieb, and M. Y. Hussaini (SIAM, Philadelphia, 1984).
19. NAG Library Mark 11, NAG, Oxford, UK.
20. S. A. ORSZAG, *J. Comput. Phys.* **37**, 70 (1980).
21. A.. T. PATERA, *J. Comput. Phys.* **54**, 468 (1984).
22. A. T. PATERA, *J. Comput. Phys.* **65**, 474 (1986).
23. T. N. PHILLIPS, *J. Comput. Phys.* **54**, 365 (1984).
24. T. N. PHILLIPS AND A. KARAGEORGHIS, *SIAM J. Sci. Stat. Comput.* **10**, 89 (1989).
25. T. N. PHILLIPS, *IMA J. Appl. Math.* **42**, 13 (1989).
26. G. GEYMONAT AND P. GRISVARD, in *Singularities and Constructive Methods for their Treatment*, edited by P. Grisvard, W. Wendland, and J. R. Whiteman (Springer-Verlag, Berlin, 1985).